Study of Improved Confinement Modes in Heliotron J*

T. Mizuuchi, F. Sano, K. Nagasaki, H. Okada, T. Minami, S. Kobayashi, S. Yamamoto, S. Konoshima, K. Hanatani, Y. Nakamura[a], K. Mukai[a], S. Kishi[a], H. Y. Lee[a], K. Minami[a], Y. Takabatake[a], N. Nishino[b], Y Nakashima[c], Y. Suzuki[d], M. Yokoyama[d]

Institute of Advanced Energy, Kyoto University, Gokasho, Uji 611-0011, Japan
[a]Graduate School of Energy Science, Kyoto University, Gokasho, Uji, Japan
[b]Graduate School of Engineering, Hiroshima University, Higashi-Hiroshima, Japan
[c]Plasma Research Center, University of Tsukuba, Tsukuba, Japan
[d]National Institute for Fusion Science, Toki, Japan

ABSTRACT

Recent studies of improved confinement in Heliotron J are reviewed. (I) Studies of the transition phenomena suggest that the change in the rotational transform (and/or its radial profile) caused by non-inductive plasma current and/or the direction of momentum input can trigger the transition in NBI plasma. Transition in NBI-only plasma has not observed in the low bumpiness configuration while it can be observed in ECH+NBI plasmas, indicating ECH affects on the transition condition in NBI plasma. Observation of edge plasma with fast cameras discovers a filamentary structure of edge plasma turbulence along the field line. The apparent rotation of this structure suggests build-up of negative E_r after the transition. (II) Studies of the global energy confinement in three configurations with different bumpiness ($\varepsilon_b(r/a = 2/3)$ = 0.01, 0.06, 0.15) were performed for NBI-only plasma. For a fixed line-averaged electron density, the highest value of the volume-averaged stored-energy W_p/V_p is obtained in the high-ε_b case. This is different from the results for ECH-only plasma, where the maximum of W_p/V_p is obtained in the medium-ε_b case. The lowest one is obtained in the low-ε_b case for both heating methods. In the ICRF minority heating experiment, the flux of minority ions with highest energy up to 34 keV can be measured only in the high bumpiness configuration, suggesting the preferable confinement of the fast-ions in the high-ε_b case. The ECCD experiments show that the direction of EC driven current is changed by the bumpiness, indicating effective control of fast-electron trapping by bumpiness tailoring. (III) A supersonic molecular beam injection (SMBI) is successfully applied to Heliotron J plasma and expands the reachable range of W_p up to about a factor 1.5 compared to the maximum one achieved so far under the conventional gas-puffing in Heliotron J.

* author's e-mail: mizuuchi@iae.kyoto-u.ac.jp

1. Introduction

The Heliotron J device is a low magnetic shear device with an $L/M = 1/4$ helical coil ($R_0 = 1.2$ m, $B_0 \leq 1.5$ T) [1, 2] based on the helical-axis heliotron concept [3]. This configuration is one of the advanced helical configuration along the quasi-omnigeneous (or quasi-isodynamic) approach. In the helical-axis heliotron concept, the bumpiness ε_b ($= B_{04}/B_{00}$) is introduced as the third measure to control the neoclassical transport in addition to the other major harmonics in the Boozer coordinates, helicity ($\varepsilon_h = B_{14}/B_{00}$) and toroidicity ($\varepsilon_t = B_{10}/B_{00}$). Here, B_{mn} is the Fourier component with the poloidal and toroidal mode numbers of m and n, respectively. From a viewpoint of the drift optimization, the bumpiness control has an important role in this concept [4]. One of the main objectives of the Heliotron J experiment is to study the configuration effects on the plasma performance only from the neoclassical transport viewpoint but also from the anomalous transport viewpoint.

The details of the Heliotron J device is described in [1, 2]. Due to the strong pitch modulation of the helical coil, the toroidal shape of the plasma looks square in the top view. The initial plasma is produced by the 70 GHz second harmonic X-mode ECH system. In the experiments described in this paper, the microwaves are launched from a top port located at a "straight section" of the square shape of the plasma. The hydrogen neutral beam (30 keV, 0.7 MW/beam-line) is injected using two tangential beam-lines facing each other (BL1 and BL2). Selecting one of the beam-line or changing the direction of the confinement field, co(Co)- or counter (CTR)-injection is performed.

The field configuration is controlled using five types of external coils, a helical coil, two individual sets of toroidal coils (TA and TB) and two sets of vertical coils (AV and IV). The major part of the field configuration is determined by the helical and toroidal coil currents. The bumpiness is mainly controlled by changing the coil current ratio of TA and TB coils, I_{TA} and I_{TB}, respectively. Trimming of other coil currents, it is possible to control ε_b within tolerable change in the other major Fourier components of the confinement field (helicity and toroidicity), the edge rotational transform $\iota(a)/2\pi|_{vac}$, the plasma volume V_p and the averaged major radius $\langle R_0 \rangle$ in the vacuum condition. On the other hand, $\iota(r)/2\pi|_{vac}$ can be controlled by mainly changing the current ratio of the helical coil to the toroidal coils.

In Heliotron J experiments, we have observed improved confinement modes (or high performance states) under several experimental conditions. This paper reviews the studies of improved confinement in Heliotron J for about the last a half decade.

2. Configuration Control for Improved Confinement

Optimization of the field configuration is an important key to obtain a higher confinement state. The configuration control studies are essential parts of the Heliotron J experiment since one of the major objectives of the Heliotron J project is to confirm the effects of the new ideas adopted in this concept and to extend the understanding of the roles of configuration parameters

in the transport, MHD activity and/or non-inductive toroidal current control along the omnigeneous optimization scenario.

The configuration control experiments have been mainly focused on two aspects; one is the effect of the rotational transform and the other is the effect of the bumpiness. The value of the rotational transform $\iota(r)/2\pi$ is essential for the good energy confinement in a low magnetic-shear device like Heliotron J. In addition, the edge rotational transform $\iota(a)/2\pi$ is also closely related with the field topology in heliotron/stellarator systems. The effects of rational surfaces have been studied in many tokamaks and helical devices not only from the viewpoint of MHD activities but also from the viewpoint of the appearance of external/internal transport barriers or enhanced confinement modes in helical devices [5].

Although the initial study of rotational transform effects on the global confinement in Heliotron J were performed for ECH-only plasma by controlling the AV filed [6], in the $\iota(a)/2\pi|_{vac}$-experiments described in this paper the control scheme by mainly changing the current ratio of the helical coil to the toroidal coils was applied, where the ratio of I_{TA}:I_{TB} was fixed to the value of the standard configuration. Figure 1 shows the $\iota/2\pi|_{vac}$-profiles and magnetic surfaces for several configurations with different $\iota(a)/2\pi$.

The study of ε_b-control effects on the bulk plasma confinement and on the behavior of fast-ions/electrons were performed selecting three different ε_b (= 0.01, 0.06, 0.15 at r/a = 2/3) configurations with almost the same rotational transform at the last closed flux surface (LCFS), $\iota(a)/2\pi|_{vac} \approx 0.56$ in the vacuum condition [7]. Figure 2 shows the radial profiles of the major Fourier harmonics for the examined three configurations.

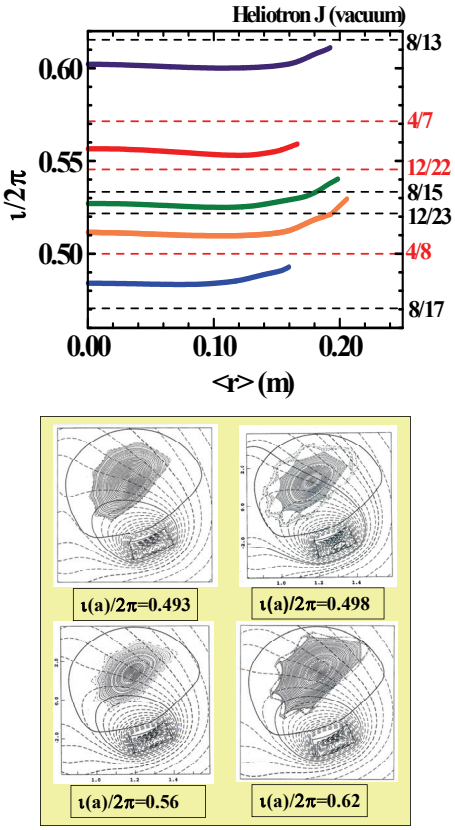

Fig. 1 Example of $\iota/2\pi|_{vac}$-profiles and magnetic surfaces

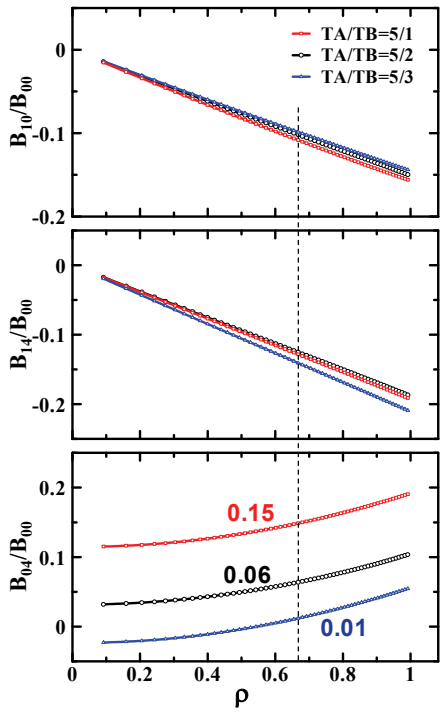

Fig. 2. Radial profiles of major Fourier harmonics for ε_b-control experiment. [7]

2.1 Spontaneous Transition Phenomena

The Heliotron J experiments have revealed the

existence of the spontaneous transition to improved confinement mode. Here the increase in the stored energy W_p and core electron density $\bar{n}_e$ is observed after the spontaneous drop of the intensity of Hα/Dα-emission. It is suggested that the reduction of the fluctuation-induced transport in the SOL and the formation of the negative E_r (or E_r-shear) near the LCFS at the transition. Recent observation of edge plasma with fast cameras discovers a filamentary structure of a peripheral plasma fluctuation along the field line and that the apparent motion of this structure changes its direction in the improved mode as shown in Fig. 3, suggesting build-up of negative E_r in the improved mode [8]. These features are similar to the characteristics of the H-mode in tokamaks. Although the edge pedestal, which characterizes the H-mode in tokamaks, has not been confirmed for the improved mode in Heliotron J, we use the name "H-mode" for this improved mode following tokamaks.

There are some reports on this kind of observation in Heliotron J for ECH-only [9, 10, 11], NBI-only plasmas [12], where plasma is sustained only by NBI after plasma initiation with a short pulse of ECH, and plasma simultaneously heated by ECH and NBI (ECH+NBI plasma) [13, 14], where the configuration effects on the accessibility condition to this transition and the "quality of the confinement" after the transition have been studied by changing the edge rotational transform $\iota(a)/2\pi$ of the vacuum field as a label of the configuration. These studies have revealed the conditions for the transition as follows:

(1) The transition is observed only for the discharges with a density higher than a critical value. The threshold line-averaged density for the transition is in the range of $\bar{n}_e = 1–2\times10^{19}$ m^{-3}.
(2) This threshold density is not sensitive to $\iota(a)/2\pi|_{vac}$ in the range of $0.493 \le \iota(a)/2\pi|_{vac} < 0.6$. For higher $\iota(a)/2\pi$-region ($\iota(a)/2\pi > 0.6$), however, some exceptional cases with low threshold density are observed.
(3) There is no clear or simple relation between the threshold density and the absorption power for a fixed field configuration,
(4) The transition has not been observed so far for (a) ECH-only plasma at $\iota(a)/2\pi = 0.493$, (b) NBI(Co)-only plasma at the low-ε_b configuration and (c) NBI(CTR)-only plasma.
(5) The density ramp-up experiments for ECH- and ECH+NBI plasmas indicate the existence

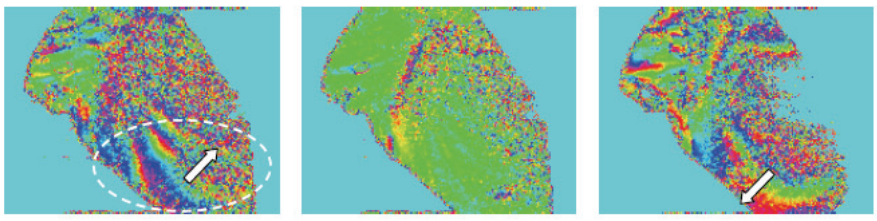

Fig. 3 Two dimensional phase images during the L-mode, the L-H transition, and the H-mode. Phase image in dashed circle region moves counterclockwise during the L-mode. During the L-H transition the motion of the phase image in dashed circle region become slow, and at the transition the rotation of the phase image stops. After the transition phase image begin to rotate but the direction is clockwise. [8]

of $\iota(a)/2\pi|_{vac}$-windows for the "high quality" transition ($\tau_E^{exp}/(f\times\tau^{ISS04}) > 1.5$) close to the low-mode rational numbers of $\iota(a)/2\pi|_{vac}$. Figure 4 shows such configuration dependence of $\tau_E^{exp}/(f\times\tau^{ISS04})$ for ECH+NBI plasmas.

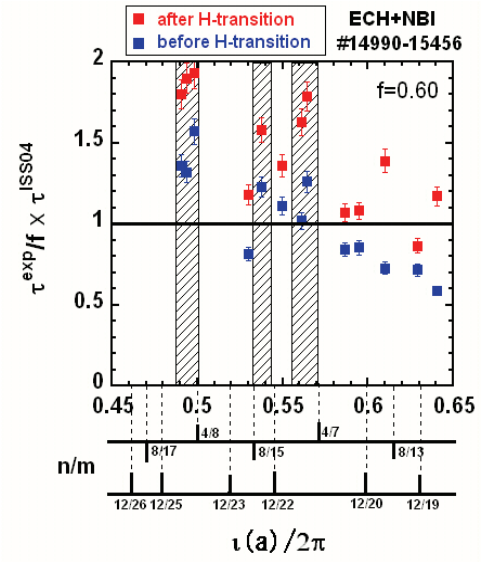

Fig. 4 Configuration effect on the normalized global energy confinement time for ECH+NBI plasma. The window for the high quality H-mode (hatching zone) is observed close to the low-mode rational numbers of $\iota(a)/2\pi|_{vac}$[5].

In these studies, $\iota(a)/2\pi|_{vac}$ is just used as a "label" of the field configuration since $\iota(r)/2\pi$ can be modified by the existence of plasma. It is considered that the increase or decrease of the rotational transform caused by non-inductive toroidal plasma current changes the edge field topology. Non-inductive current can be driven by the pressure gradient (bootstrap current), electron cyclotron current drive (ECCD) and neutral beam current drive (NBCD), etc. In the Heliotron J experiments, it is experimentally confirmed that the direction and/or intensity of bootstrap current and ECCD current depends on the field configuration [15, 16]. The tangential NBI system can also control the direction and intensity of NBCD current by selecting the beam lines and by controlling the injection power. In addition, the rotational transform can be affected through the finite-β effect. Actually, the shift of the divertor plasma distribution during a single discharge has been observed [17], indicating the modification of the edge field structure (or topology).

Since low order rational values of the rotational transform are considered to be associated with both improved confinement and the role of the magnetic shear is also discussed [5], it is interesting to investigate the effect of the change in the field topology or $\iota(r)/2\pi$ on the transition windows and its "quality of enhancement".

Comparative experiments between co- and counter-injection NBI-only plasmas show the difference in the accessibility to the transition. Between these two injection cases, the direction of no-inductive current is different. As mentioned before, the transition has never been observed so far in NBI(CTR)-only plasma, suggesting the importance of $\iota(r)/2\pi$ change caused by non-inductive plasma current.

NBI(Co)-only plasma experiments in Heliotron J show a strong dependence of the toroidal plasma current I_p on the occurrence of the transition [12]. For NBI(Co)-only plasmas with $\bar{n}_e \approx 1.5\text{-}2\times10^{19}$ m^{-3}, the transition happened when the toroidal current reached a critical I_p value, which did not depend on the injection power P_{inj} as shown in Fig. 5. Here the plasma current mainly consists of the bootstrap and NBCD currents, and the poloidal field induce by this net current increases $\iota(a)/2\pi$, i.e. "additive" current. The intensity of this critical current depends on the configuration, $\iota(a)/2\pi|_{vac}$ and/or the bumpiness. Figure 6 shows the $\iota(a)/2\pi|_{vac}$ dependence of

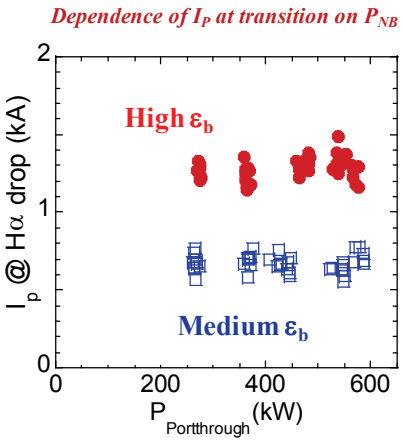

Fig. 5 P_{inj}-dependence of I_p observed at the transition for NBI(Co)-only plasma in high- and medium-ε_b configurations. $\bar{n}_e \approx 1.5\text{-}2\times10^{19}$ m^{-3} [12].

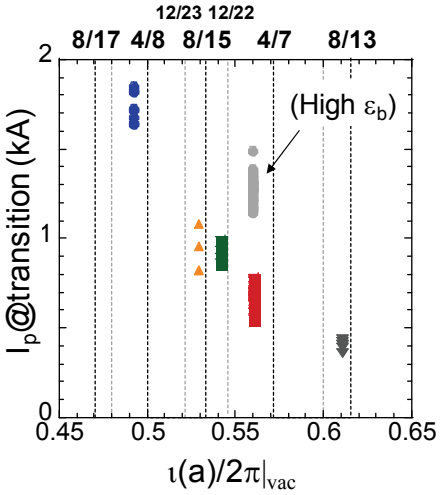

Fig. 6 $\iota(a)/2\pi|_{vac}$-dependence of I_p at the transition. NBI(Co)-only (P_{inj} = 0.25-0.6 MW) $\bar{n}_e \approx 1.5\text{-}2\times10^{19}$ m^{-3}.[12].

I_p at the transition. As shown in the figure, the critical current exists for all configurations and its value systematically decreases as increase of $\iota(a)/2\pi|_{vac}$. In the high-ε_b configuration at $\iota(a)/2\pi|_{vac} \approx 0.56$, the transition can be observed and the plasma current at the transition is higher than that in the medium-ε_b configuration. In the low-ε_b configuration, however, the transition could not be observed at least in this density and power range.

If the net toroidal current itself is a key parameter for the transition, the similar relation of I_p and $\iota(a)/2\pi|_{vac}$ should be observed for different heating schemes. Figure 7 shows I_p at the transition for ECH-only plasma, where data from density ramp-up experiments are plotted. For the low-ε_b configuration, where the transition can be observed for ECH-only plasma, data from low density ($\sim 0.3\times10^{19}$ m^{-3}) ECCD experiments are also plotted. Except for this low density ECCD case, the observed plasma current is considered to be come from the bootstrap current. The data for the standard configuration (medium-ε_b) the intensity of I_p is in almost the same range as that observed for NBI(Co)-only plasma. For lower $\iota(a)/2\pi|_{vac}$ configuration, however, the intensity of I_p for ECH-only plasma is clearly low compared to that for NBI(Co)-only plasma. Although the present data set is limited to only two $\iota(a)/2\pi|_{vac}$ conditions, a strong $\iota(a)/2\pi|_{vac}$ dependence is not shown in Fig. 7. The ε_b-dependence of I_p at =0.56 is consistent with the

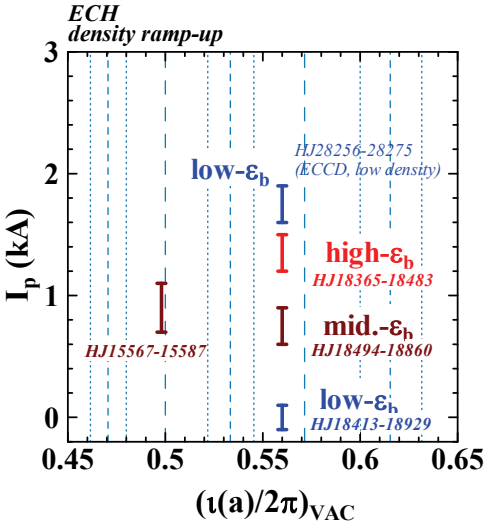

Fig. 7 I_p at the transition for ECH-only plasma in several configurations. Data from density ramp-up experiments are plotted. For the low-ε_b configuration, data from low density ECCD experiments are also plotted.

ε_b-dependence of the bootstrap current [16].

The $\iota(a)/2\pi|_{vac}$-dependence of I_p observed for ECH+NBI(Co) combination heating plasma is shown in Fig. 8, where the data from density ramp-up experiments are plotted. In this case, almost the same dependence is observed as that for NBI(Co)-only plasma, although I_p for the ECH+NBI(Co) plasma is higher than that for NBI(Co)-only plasma.

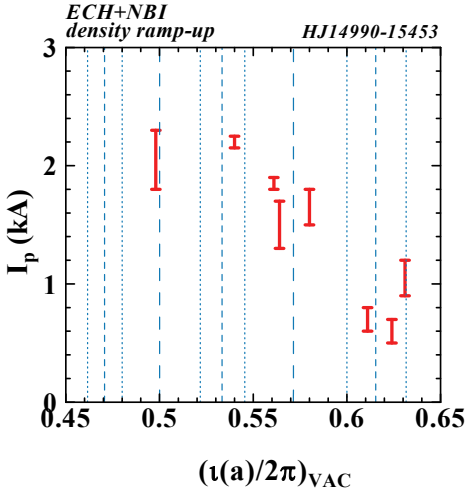

Fig. 8 I_p at the transition for ECH+NBI(Co) plasma in several configurations. Data from density ramp-up experiments are plotted.

The observed difference in the role of I_p among ECH- and (ECH+)NBI(Co)-plasmas would cause three probable ideas on the transition condition problem: (1) transition mechanism (physics) is different between ECH and NBI plasmas, (2) the plasma current is not a primary factor in the transition for all cases, (3) the important factor is not the intensity of net current but the current profile. As for the third possibility, HINT-2 calculations of the equilibrium flux surfaces by assuming a pressure profile with different current profiles show that not only the intensity of net current and its direction but also the current profile can cause severe deformation of the flux surfaces [17]. Even for ECH-only plasma with the density lower than the usual threshold, the transition can be observed when the EC driven "additive" current is high enough as shown in Fig. 7. Therefore, as for the effect of the plasma current, we have to check the current profile or actual change of the flux surface. This is an important future work.

On the other hand, in tokamaks, plasma rotation is also considered as one of key parameters to the transition. From this point of view, the fact that the transition could not be observed in NBI(CTR)-only plasma might indicate the importance of momentum input by NB.

Finally, it is interesting to note that the bumpiness control experiments revealed that the transition has not been observed so far in NBI(Co)-only plasma at the low-ε_b configuration as mentioned before, while the transition is observed for ECH-only and ECH+NBI(Co) plasmas in the same low-ε_b configuration. This observation might indicate that ECH could relax the condition of the transition in NBI plasma. It is well known the ECH pulse causes the density pump-out phenomena. The change in the plasma profile caused by this process might relax the condition of the transition in NBI-plasma. More detailed studies based on the profiles of density, temperature and electric potential are necessary.

2.1 Bumpiness Control

The study of bumpiness control effects on the bulk plasma confinement and on the behavior of fast-ions/electrons were performed selecting three different bumpiness configurations with the same rotational transform at the last closed flux surface (LCFS), $\iota(a)/2\pi \approx 0.56$ in the vacuum condition [7].

As for the ε_b-effect on the fast-ion behavior, which was examined by superimposing an NBI or ICRF pulse on ECH target plasmas, the experiments indicate that the higher ε_b configuration is preferable not only for the confinement of high-pitch angle fast-ions [18, 19], which are generated by ICRF, but also for that of low-pitch angle ones [20, 21], which come from the tangential NBI. The preferable behavior of high-pitch angle particles in the high-ε_b configuration is qualitatively consistent with the drift optimization viewpoint. In addition, a wide configuration scan in ECCD experiments in Heliotron J also indicates the effectiveness of ε_b-control to change the ripple trapping efficiency of higher energy electrons accelerated by electron cyclotron resonance heating [22].

Although the observed ε_b-dependence of the confinement of low-pitch angle fast-ions is preferable for plasma heating by tangential NBI, its mechanism is not clear. Further experiments will be necessary to understand this ε_b-dependence.

On the other hand, as for the ε_b-effects on the global energy confinement, the dependence seems not so simple, where plasma turbulence has an important role in the transport.

Figure 9 shows the volume averaged stored energy for ECH-only plasma as a function of $\bar{n}_e$, where the injection power of microwaves is in the range of 0.29-0.32 MW. The plasma volume in the vacuum condition is used here although the transition is included in the data set. This figure shows that the plasma performance in the low-ε_b configuration is clearly low in the whole range of density compared to those in the other configurations. Although the difference between medium-ε_b and high-ε_b configurations is not clear for low density region, the plasma performance is better in the medium- ε_b configuration than that in the high-ε_b configuration. In higher density region, the transition is easily obtained in the medium-ε_b configuration, but not in the high-ε_b configuration [7]. The increase of W_p due to the transition might cause the clear difference in W_p/V_p between medium- and high-ε_b cases. Even in the low-ε_b configuration, the transition was

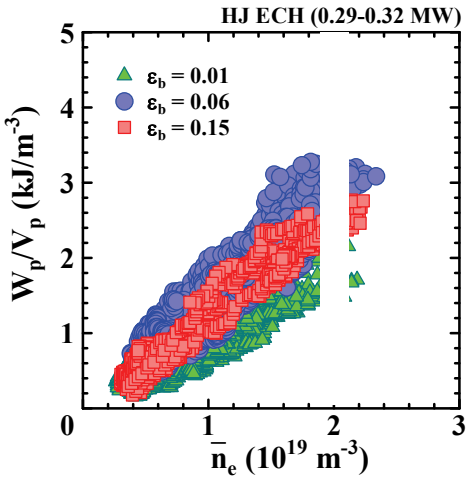

Fig. 9 Comparison of ε_b-effect on the plasma performance. (ECH-only plasma, density ramp-up experiment)

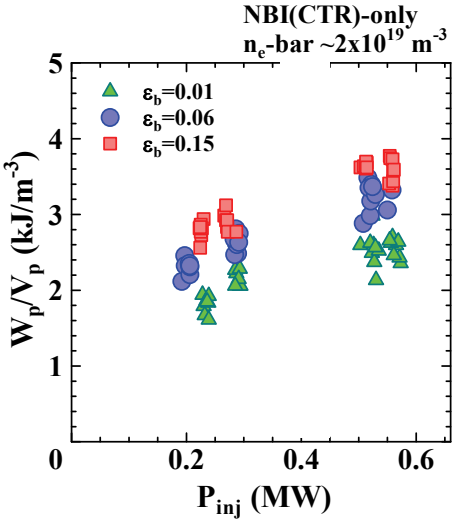

Fig.10 Comparison of ε_b-effect on the NBI(CTR)-only plasma performance.

frequently observed in higher density region and resulted in data points close to the data for the medium-ε_b case in the figure.

On the other hand, different dependence is observed for NBI(CTR)-only plasma. Figure 10 shows the volume averaged stored energy as a function of the injected NB power. In this experiment, the density is controlled to $\bar{n}_e \approx 2\times10^{19}$ m^{-3}, and the counter NB injection is selected to avoid the complexity relating to the transition phenomena [21]. In this density, about 30% of the injected power is lost as the shine-through. The value of W_p/V_p in the low-ε_b configuration is lower than those in the medium- and high-ε_b cases. This is the same tendency as that for ECH-only plasma. However, the configuration which shows the highest W_p/V_p value is not the medium-ε_b one but the high-ε_b one for NBI(CTR)-only plasma.

Although we should take care the difference of the experimental scheme between these ECH-only and NBI(CTR)-only experiment, these observations suggest the possibility of different ε_b-dependence of the global energy confinement between ECH-only and NBI(CTR)-only plasmas. More experimental studies is necessary to make it clear the role of the bumpiness control in the anomalous and neoclassical transport, and, therefore, in the confinement improvement.

3. Fueling Control

The gas fueling control is one of the most important factors to obtain a high density and good performance plasma from two aspects; (1) the profile control of the core plasma density through the controlled penetration depth of neutral particles and (2) the reduction of neutral particles in the peripheral region. It is well known in tokamaks that the excess neutral gas can degrade the plasma performance. Although the optimization of this fueling method for the Heliotron J experiment is in progress, the stored energy reached ~ 4.5 kJ in a combination heating condition of ECH (~ 0.35 MW) and NBI (~ 0.6 MW), which is about 50 % higher than the maximum one achieved so far under the conventional gas-puffing in Heliotron J [23] as shown in Fig. 11. Here, $H\alpha^{\#11.5}$ is the Hα-intensity at the same toroidal section as the SMBI port and $H\alpha^{\#3.5}$ is that at the almost opposite position along the torus. The sharp increase in $H\alpha^{\#11.5}$ indicates the SMBI is fired.

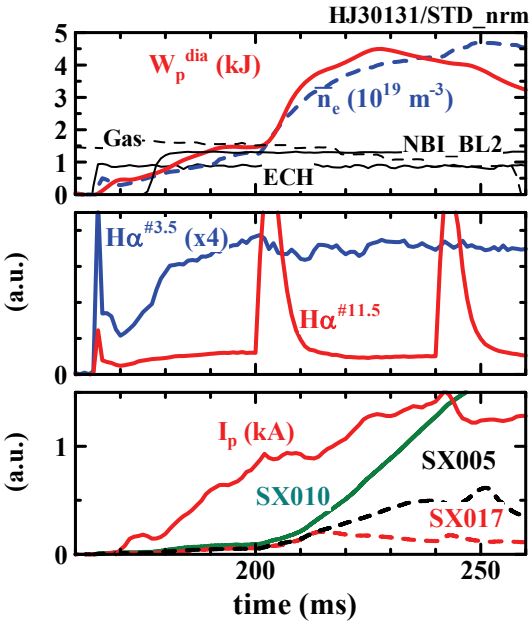

Fig. 11 Time traces of $\bar{n}_e$, W_p, Hα at two different sections, I_p and I_{SX} for an ECH+NBI discharge with SMBI.

In Fig. 11, note that Ha#3.5 is dropped at the first SMBI timing, perhaps indicating the occurrence of the transition. It is interesting to

investigate whether SMBI can trigger the transition, but this is future works.

In order to use the SMBI method for more improving plasma performance or expanding the attainable plasma parameter range, more detailed studies and refinement of the SMBI system including an effective pumping system or recycling control are necessary. The optimization of this fueling technique for the Heliotron J experiment is in progress.

4. Summary

Recent studies of improved confinement in Heliotron J are reviewed.

(I) Transition to improved confinement:

- Observation of edge plasma with fast cameras discovers a filamentary structure of edge plasma turbulence along the field line. The apparent poloidal rotation of this structure changes its direction before and after the transition. The direction during the H-mode suggests build-up of negative E_r after the transition.
- Studies of the transition phenomena in NBI plasma suggest that the change in the rotational transform (and/or its radial profile) caused by non-inductive plasma current and/or the direction of momentum input can trigger the transition in NBI plasma.
- Even in low density ECH-only plasma lower than the threshold density, the transition can be observed when the EC driven "additive" current is high enough.
- Transition in NBI-only plasma has not observed in the low bumpiness configuration while it can be observed in ECH-only or ECH+NBI plasmas, indicating that ECH could relax the condition of the transition in NBI plasma.

(II) Effects of Bumpiness Control

- Studies of the global energy confinement in three configurations with different bumpiness ($\varepsilon_b(r/a = 2/3) = 0.01, 0.06, 0.15$) were performed for NBI-only plasma.
- For a fixed $\overline{n}_e$, the highest value of W_p/V_p is obtained in the high-ε_b case. This is different from the results for ECH-only plasma, where the maximum of W_p/V_p is obtained in the medium-ε_b case.
- The lowest one is obtained in the low-ε_b case for both heating methods.
- Studies of bumpiness effects on the behavior of fast-ions (H^+) generated by ICRF minority heating or fast-electrons generated by ECH have progressed.
- In the ICRF experiment, the ion-flux with highest energy up to 34 keV can be measured only in the high bumpiness configuration, suggesting the preferable confinement of the fast-ions in the high-ε_b case.
- The ECCD experiments show that the direction of EC driven current is changed by the bumpiness, indicating effective control of fast-electron trapping by bumpiness tailoring.

(III) Fueling control

- A supersonic molecular beam injection (SMBI) is successfully applied to Heliotron J plasma and expands the reachable range of W_p up to about a factor 1.5 compared to the maximum one achieved so far under the conventional gas-puffing in Heliotron J.
- For further improvement of plasma performance and expanding the attainable plasma parameter range, more detailed studies and refinement of the SMBI system and developing an effective pumping system or recycling control are necessary.

The configuration parameter ($\iota/2\pi$, ε_b) range, which has been surveyed so far, is limited. Experiments in the expanded investigation range in ($\varepsilon_t/\varepsilon_h$, $\varepsilon_b/\varepsilon_h$)-space with different iota values are proposed.

Acknowledgement

The authors are grateful to the Heliotron J supporting group for their excellent arrangement of the experiments. This work is performed with the support and under the auspices of the Collaboration Program of the Laboratory for Complex Energy Processes, IAE, Kyoto University, the NIFS Collaborative Research Program (*NIFS04KUHL001-005*, et al.), the NIFS/NINS project of Formation of International Network for Scientific Collaborations, JSPS-CAS Core University Program as well as the Grant-in-Aid for Sci. Research.

References

[1] F. Sano, et al., J. Plasma Fusion Res. Ser. **3**, 26 (2000).
[2] T. Obiki, et al., Nucl. Fusion **41**, 833 (2001).
[3] M. Wakatani, et al., Nucl. Fusion **40**, 569 (2000).
[4] M. Yokoyama, et al., Nucl. Fusion **40**, 261 (2000).
[5] for example, E. Ascasíbar, et al., Plasma Fusion Res. **1**, 001 (2006).
[6] T. Obiki, et al., J. Plasma Fusion Res. Ser.**3**, 288 (2002).
[7] T. Mizuuchi, et al. Fusion Sci. Tech. **50**, 352 (2006).
[8] N. Nishino, et al., J. Nucl. Mater. **390-391** 432 (2009).
also, in this workshop, C09.
[9] F. Sano, et al., 30th EPS Conference on Contr. Fusion and Plasma Phys.
(St. Petersburg, 2003), ECA Vol.27A, O-2.2A.
[10] F. Sano, et al., J. Plasma Fusion Res. **79**, 1111 (2003).
[11] F. Sano et al., Fusion Sci. Tech. **46**, 288 (2004)
[12] S. Kobayashi, et al., 11th IAEA-TCM on H-mode Phys. Trans. Barrier
(Tsukuba, 2007) P4-03.
T. Mizuuchi, et al., Joint Conf. "17th Int. Toki Conf. on Phys. Flows & Turbulence
in Plasmas" and "16th Int. Stellarator/Heliotron Workshop" (Toki, 2007) O-02.
[13] F. Sano, et al., Nucl. Fusion **45**, 1557 (2005).
[14] T. Mizuuchi, et al., Plasma Sci. Tech. **6**, 2371 (2004).
[15] G. Motojima, et al., Fusion Sci. Tech. **50**, (2006).
[16] G. Motojima, et al., Nucl. Fusion **46**, (2007).
[17] T. Mizuuchi, et al., Nucl. Fusion **47**, 395 (2007).
[18] H. Okada, et al., Fusion Sci. Tech. **50**, 287 (2006).
[19] H. Okada, et al., in 18th Int. Toki Conf. (Toki, 2008) I-03.
[20] S. Kobayashi, et al., IAEA-CN-116/EX/P4-41 (2004).
[21] S. Kobayashi, et al., 22nd IAEA Fusion Energy Conference (Geneva, 2008) EX/P5-13.
[22] K. Nagasaki et al., 22nd IAEA Fusion Energy Conference (Geneva, 2008) EX/P6-15.
submitted to Nucl. Fusion.
[23] T. Mizuuchi, et al., in this workshop, P01-17.